10.2 INTERACTIVE IMPACT OF CCN, GCCN, AND IFN ON SNOWFALL OVER THE PARK RANGE

Stephen M. Saleeby* and William R. Cotton

Department of Atmospheric Science, Colorado State University, Fort Collins, CO

1. INTRODUCTION

The Park Range of Colorado receives the majority of its annual precipitation in the form of snow during the winter months. This north/south oriented mountain range is generally aligned orthogonally to the westerly mean flow that accompanies most synoptic mid-latitude cyclones over the western U.S. (see Fig. 1). In the absence of blocked flow, deep lifting of a near-surface airmass from the west can be transported over the crest of the Park Range. This deep lifting along the slope provides for enhanced condensate production and surface snowfall that would otherwise remain limited. In addition to orographically generated snowfall, the strong cross-barrier pressure gradient and upslope wind tends to produce an orographic cloud with supercooled liquid water (Rauber et al., 1986; Borys et al., 2000). These supercooled cloud events are often observed during the winter months at the Desert Research Institute's Storm Peak Lab (SPL). SPL is a high-altitude research facility located atop Mt. Werner (~3210m MSL) near Steamboat Springs, CO (Borys and Wetzel, 1997).

A seeder-feeder mechanism, involving the sedimentation of higher altitude snow crystals through the low-level orographic cloud, produces greater precipitation amounts near mountaintop due to ample riming of cloud droplets in the lowest 2 km (Rauber et al., 1986). This low-level riming process enhances the precipitation efficiency, such that, the amount of rime has been shown to comprise from 20-50% of the final snow mass that reaches the surface (Borys et al., 2003). Enhanced riming will increase the mass of snow crystals as well as the fall speed; this increases the likelihood of higher snow deposits along windward slopes (Hindman, 1986). Slower falling, unrimed snow crystals are more likely to fall on the leeward slopes where subsidence leads to evaporation, a reduction in total surface snowfall, and disappearance of the "feeder" cloud.

While topography and riming may result in locally enhanced snowfall, intrusions of high concentrations of pollution aerosols can modify the condensate fields. Additions of sulfate-based cloud condensation nuclei (CCN) and giant-CCN (GCCN) can modify the liquid droplet spectra in the supercooled orographic feeder cloud, and ice forming nuclei (IFN) can modify the ice crystal spectra in the overlying seeder cloud. Changes in the size distributions will impact the snow riming efficiency (Hindman, 1994). Borys et al. (2000) found that increased aerosol concentrations (CCN) suppress formation of larger cloud droplets and reduce riming of cloud droplets by ice hydrometeors. However, little is known of the impact of GCCN or IFN within this type of orographic system.

This study examines the relative impacts of CCN, GCCN, and IFN number concentrations on total snowfall and snowfall distributions near the Park Range of Colorado. This is accomplished with use of a mesoscale model to produce high resolution simulations of winter orographic snowfall events.

Corresponding author address: Stephen M. Saleeby, Colorado State Univ., Atmos. Sci. Dept., Fort Collins, CO 80523; e-mail: smsaleeb@atmos.colostate.edu

2. MODEL DESCRIPTION

The Colorado State University - Regional Atmospheric Modeling System (RAMS) Version 4.3 has been utilized for a set of sensitivity simulations with varying amounts of CCN, GCCN, and IFN number concentration. The non-hydrostatic, compressible version of RAMS is configured on an Arakawa-C grid and sigma-z terrain-following coordinate system (Cotton et al., 2003). For these simulations, the model uses two-way nesting with a nested 4-grid arrangement centered over Colorado. The outer grid-1 covers the continental United States with 60km grid spacing (62 x 50 grid pts), grid-2 covers Colorado and the adjacent surrounding states with 15km grid spacing (54 x 50 grid points), grid-3 encompasses much of Colorado with 3km grid spacing (97 x 82 grid points), and grid-4 covers the north-south oriented Park Range from the cities of Hayden to Walden with 750m grid spacing (114 x 114 grid points) (Fig. 1). Within each grid there are 40 vertical levels with a minimum of 75m grid spacing. The model uses vertical grid stretching with a stretch ratio of 1.12 and a maximum vertical grid spacing of 750m.

The RAMS model contains a highly sophisticated, state-of-the-art microphysics package that predicts on two-moments of the hydrometeor distributions (mixing ratio and number concentration) for rain, pristine ice, snow, aggregates, graupel, and hail (Meyers et al. 1997). Saleeby and Cotton (2004) extended the two-moment approach to the cloud droplet distribution via a parameterization for the formation of cloud droplets from activation of CCN and/or GCCN within a lifted parcel. The Lagrangian parcel model of Heymsfield and Sabin (1989), was utilized to determine the percent of user-specified nuclei that would activate and grow by condensation into cloud droplets for a given ambient temperature, vertical velocity, and median radius of the aerosol distribution. Saleeby and Cotton (2008) introduced a binned approach to riming within the bulk microphysics framework in which realistic collection efficiencies are used compute the collision-coalescence between ice crystals and cloud droplets. The hydrometeor gamma distributions are temporarily

decomposed into 36 size bins for riming computations of all possible size interactions. This method is highly beneficial in winter orographic simulations, and is much improved over the bulk riming method which applied a single collection efficiency value to the full size distribution. The CCN and GCCN number concentrations (N_{CCN} and N_{GCCN}, respectively) were initialized horizontally homogeneous with a vertical profile that decreases linearly with height up to 4km AGL. Initial surface N_{CCN} were specified at 100 and 1900 cm^{-3} and N_{GCCN} of 0.00001 and 0.5 cm^{-3}. The lower value is meant to represent clean conditions and the upper value, polluted conditions. The minimum concentration allowed at any location was 100 cm^{-3} for CCN and 0.00001 cm^{-3} for GCCN. The aerosol concentrations are represented on a poly-disperse lognormal distribution with a median radius for CCN of 0.04μm and GCCN of 3.0μm. As a simple source/sink function, CCN and GCCN are depleted upon droplet nucleation and replenished upon droplet evaporation. IFN are represented as a density weighted decaying concentration profile of $N_{IFN} \times \rho^{5.4}$ with maximum number concentration of 100 L^{-1}. The maximum number of IFN to nucleate is dependent upon supersaturation with respect to ice and is given as:

$$\text{Meyers} = N_{IFN} \times \rho^{5.4} \times \exp\left(12.96 * (S_i - 0.40)\right) \text{ or}$$

$$\text{DeMott} = N_{IFN} \times \rho^{5.4} \times \exp\left(12.96 * (S_i - 0.40)\right) \times 10^{(-4.077 * S_i + 0.0975)}.$$

These ice nucleation formulas provide the maximum number of ice crystals to nucleate via deposition condensation freezing upon IFN. New ice crystal formation via IFN only occurs if the Meyers or DeMott number concentration is greater than the existing concentration of pristine ice crystals. They provide an upper limit to the number of ice crystals forming in this manner. Both formulas are derived from curve fits to data observed from ice nucleus counters. The DeMott formula indicates less ice forming activity than the Meyers formula.

An ensemble of 42hr simulations were conducted for a heavy riming, heavy snowfall event from February 11-13, 2007. The 32km North American Regional Reanalysis was used for model initialization and nudging of the lateral boundaries.

3. IMPACTS OF POLLUTION AEROSOLS

a. CCN Effect

Aerosol particles in the sub-micron range with a dry median radius around 0.04 μm are small enough that high supersaturation is required to overcome curvature effects and become activated. High N_{CCN} leads to high concentrations of small droplets, whereas, low N_{CCN} results in fewer, larger droplets. Smaller droplets have much smaller collection efficiencies, and are less likely to be rimed and contribute to the total surface water. From figure 2, the simulations with the higher N_{CCN} resulted in suppressed snow water equivalent (SWE) on the windward slopes and increased SWE on the leeward slopes. There is not simply a reduction in precipitation everywhere due to the pollution, but rather a re-distribution due to enhanced downstream advection of the more lightly rimed, slower falling crystals in the polluted case. The CCN effect on snowfall exhibits the same trend for different background values of N_{GCCN}, although the increase in N_{CCN} results in a greater modification of snowfall for high N_{GCCN}. GCCN produce larger initial droplets that have a relatively high riming efficiency. The introduction of a high N_{CCN} counters the GCCN effect by reducing mean droplet size and the degree of riming. Since higher N_{GCCN} lead to more riming and greater snowfall, the addition of CCN have a greater impact when GCCN are numerous.

The time series plots of domain summed microphysical quantities in figure 3 help to clarify the competing cloud growth and precipitation processes that vary with aerosol concentrations. For the increase in N_{CCN}, at both low and high N_{GCCN}, the magnitude of riming is diminished, but more so for greater N_{GCCN}. As a result, the amount of existing cloud LWC increases for increasing N_{CCN}, regardless of N_{GCCN}. The curves of cloud nucleation and vapor deposition have opposite trends and are closely inter-related with riming. If N_{CCN} rises, droplets become numerous but smaller; their lifetime in the cloud is longer since they rime less effectively. The persistence of numerous droplets increases the surface area available for vapor growth. As such, the vapor deposition process utilizes excess vapor beyond supersaturation, and the nucleation of new droplets diminishes.

The total domain-summed precipitation change on grid-4, due to an increase in N_{CCN} from 100 to 1900 cm^{-3}, was only 0.7% at low N_{GCCN} and -0.8% at high N_{GCCN}. These domain-wide changes are quite small and exhibit an inconsistent trend in the sign of change.

b. Giant - CCN Effect

The impact of GCCN is nearly opposite to that of CCN. The 3μm radius is large enough that curvature effects offer little inhibition for activation and droplet nucleation. The parcel model results for GCCN suggested that nearly all available GCCN will support new droplet formation even at modest supersaturation. Furthermore, they nucleate into droplets with considerable initial size, such that riming of these droplets is immediately active. Compared to CCN, further growth by vapor deposition is unnecessary to reach a minimum size prior to riming.

Figure 4 displays the change in SWE precipitation for the given increase in N_{GCCN} at both low and high background values of N_{CCN}. Along the Park Range, this plot depicts nearly a mirror image of the CCN effect. Here the precipitation is increased along the windward slope and decreased along the leeward slope. This is primarily a function of the riming by the seeder-feeder process. Newly formed droplets in the large cloud droplet mode, via GCCN, are readily rimed. While an addition of number concentration would tend to reduce the average droplet size, it is not sufficient to squelch the riming process. Newly formed large droplets

offer more sites for riming which leads to increased surface deposition.

The introduction of a few large droplets also increases the overall cloud droplet self-collection process and tends to broaden the droplet distribution. Feingold et al. (1999) recognized this GCCN effect for warm rain clouds. This has self-reinforcing ramifications, whereby the broadened distribution lends itself toward further droplet growth by self-collection resulting from greater droplet differential fall speeds.

From figure 4, the GCCN effect is greatest in this winter orographic cloud environment at low N_{CCN}. This is contrary to traditional thought for the injection of GCCN in warm rain clouds, but here we are dealing with lower supersaturation, typically smaller droplets, and precipitation modification primarily by riming. Looking at the microphysical time series in figure 3, the amount of riming is maximized at low N_{CCN} and high N_{GCCN}. While the addition of N_{GCCN} in the high N_{CCN} environment helps to stimulate droplet self-collection and riming, perhaps only a limited number of droplets begin to reach the size needed for heavy riming. At low N_{CCN} many of the droplets may already be of riming size. An additional insurgence of GCCN may be enough to trigger the collection needed for growth to optimal riming size. Both the number concentration and size of droplets determine how much riming occurs in-cloud.

The GCCN effect on the seeder-feeder process is to modify the degree of riming. Heavy riming leads to more dense snow crystals and formation of graupel. The model microphysics uses a heat budget computation to determine the amount of rimed water remaining unfrozen. If enough riming occurs to prevent instantaneous freezing, then part of the snow mass distribution is transferred to the graupel category. This category has a greater density and offers less drag, and therefore, it has a greater fall speed. The higher density ice particles deposit further upstream than the low density particles. Figure 5 displays the difference in accumulation of the snow + aggregate SWE and the graupel SWE for the given increase in N_{GCCN}. Over much of the Park Range, the aggregate mass is reduced while the graupel accumulation is enhanced, especially along the windward slope and ridge. The net difference produces a greater concentration of total SWE along the windward slope.

The total domain-summed precipitation change due to an increase in N_{GCCN} from 0.00001 to 0.5 cm^{-3} was 3.2% at low N_{CCN} and 1.6% at high N_{CCN}. The enhancement of GCCN displays an increasing trend in total precipitation, but more so, at lower background N_{CCN} values. Perhaps these larger hygroscopic particles could be used effectively in wintertime weather modification.

c. IFN Effect

The influence of IFN is quite different from that of CCN or GCCN. Figure 6 displays the precipitation difference when increasing IFN nucleation from the DeMott formula to the Meyers formula for both a background N_{CCN} maximum of 100 and 1900 cm^{-3}. GCCN were few for these simulations. It is immediately apparent that altering the IFN nucleation rate from the given vertical distribution has a substantially reduced impact compared to CCN and GCCN. The precipitation modification is generally less than 2 mm, aside from a few locations along the Park Range. The changes that do occur are mostly along the sloped terrain where enhanced upward motion near the surface would tend to trigger new ice formation near the orographic cloud.

Figure 7 shows the domain summed time series of riming and ice vapor deposition for the IFN experiments. The degree of riming exhibits very little variation due to a change in IFN nucleation. Since riming is the primary method of precipitation modification by aerosols in this orographic cloud environment, small changes in riming tend to lead to small changes in total precipitation. The time series of ice crystal vapor deposition, however, differ substantially. The more active Meyers nucleation produces greater numbers of crystals, and therefore, a greater number of sites and surface area for ice vapor growth. This increase is apparent at both low and high N_{CCN}, though, the change is greatest for high N_{CCN}. At high N_{CCN} concentration (high cloud droplet number concentration), it is likely that the increase in ice nucleation leads to ice vapor growth in a Bergeron-Findeisen regime in which the smaller cloud droplets more readily evaporate and allow that vapor to be consumed by the ice crystals. This process may account for the modest precipitation increases near the ridge and region of orographic cloud.

The total domain-summed precipitation change due to an increase in N_{IFN} from the DeMott value to the Meyers value was 0.8% at low N_{CCN} and 1.9% at high N_{CCN}. The enhancement of IFN displays a modest increasing trend in total precipitation, but more so, at higher background N_{CCN} values.

4. CONCLUSIONS

The CSU-RAMS model has been used in the current study to investigate the relative impacts of CCN, GCCN, and IFN pollution aerosols on orographically enhanced wintertime precipitation. The nested, fine resolution grid with 750m grid spacing was focused over the north-south aligned Park Range of Colorado. RAMS was chosen for this study because of its parameterization for the activation of aerosols and nucleation of cloud droplets (Saleeby and Cotton, 2004), as well as its newly implemented binned scheme for simulating the riming growth process of frozen hydrometeors (Saleeby and Cotton, 2008).

In this study, a set of 42 hour simulations were run for a heavy riming and heavy orographic snowfall event beginning 0000 UTC on 11 Feb 2007. RAMS was run for the duration of these cases with varying profiles of maximum CCN GCCN concentrations and with low and high IFN nucleation rates.

In summary, the impact of increasing the CCN concentration leads to a shift in snowfall distribution from the windward slope to the leeward slope due to a reduction in rime growth of ice crystals. An increase in CCN leads to an increase in droplet number but

reduction in droplet size. Smaller drops are rimed less effectively, which leads to smaller and less dense ice crystals. The lighter crystals tend to advect further downstream prior to surface deposition. Thus, the blowover effect shifts the snowfall distribution downstream. An increase in GCCN tends to enhance the riming process due to production of large cloud droplets that are readily rimed by snow crystals. Increased riming leads to faster surface deposition, and thus, a shift in snow distribution that favors increased precipitation on the windward slope. An increase in IFN nucleation rate has a small impact on total precipitation compared to that of CCN or GCCN. The increase in ice crystal nucleation, however, tends to slightly modify precipitation near areas of supercooled cloud water where the Bergeron process may be active enough to allow enhanced crystal growth by vapor deposition at the expense of the cloud droplets. The domain-wide precipitation modification was greatest for the GCCN, with a direct increase in precipitation associated with higher GCCN number concentrations. This domain summed trend was also present for an increase in IFN, but was inconclusive for CCN.

Acknowledgements: This research was supported by the National Science Foundation under grant ATM-0451439 and by UCAR-NCAR-COMET under grant S04-44700. Logistical assistance from the Steamboat Ski and Resort Corporation is greatly appreciated. The Desert Research Institute is an equal opportunity service provider and employer and is a permittee of the Medicine-Bow and Routt National Forests.

5. REFERENCES

Borys, R.D. and M.A. Wetzel, 1997: Storm Peak Laboratory: A research, teaching, and service facility for the atmospheric sciences. *Bull. Am. Meteorol. Soc.*, **78**, 2115–2123.

_____, D.H. Lowenthal, and D.L. Mitchell, 2000: The relationships among cloud microphysics, chemistry, and precipitation rate in cold mountain clouds. *Atmos. Environ.*, **34**, 2593-2602.

_____, _____, S.A. Cohn, and W.O.J. Brown, 2003: Mountaintop and radar measurements of anthropogenic aerosol effects on snow growth and snowfall rate. *Geo. Res. Lett.*, **30**, 1538, doi:10.1029/2002GL016855.

Hindman, E.E., M.A. Campbell, and R.D. Borys, 1994: A ten-winter record of cloud-droplet physical and chemical properties at a mountaintop site in Colorado. *J. Appl. Meteor.*, **33**, 797-807.

Hindman, E.E., 1986: Characteristics of supercooled liquid water in clouds at mountaintops in the Colorado Rockies. *J. Clim. Appl. Meteor.*, **25**, 1271-1279.

Heymsfield, A. J., and R. M. Sabin, 1989: Cirrus crystal nucleation by homogeneous freezing of solution droplets. *J. Atmos. Sci.*, **46**, 2252-2264.

Rauber, R.M., L.O. Grant, D. Feng, and J.B. Snider, 1986: The characteristics and distribution of cloud water over the mountains of northern Colorado during wintertime storms. Part II: Spatial distribution and microphysical characteristics. *J. Climate Appl. Meteor.*, **25**, 489-504.

Saleeby, S.M., and W.R. Cotton, 2004: A large droplet mode and prognostic number concentration of cloud droplets in the Colorado State University Regional Atmospheric Modeling System (RAMS). Part I: Module descriptions and supercell test simulations. *J. Appl. Meteor.*, **43**, 182-195.

_____, and _____, 2008: A binned approach to cloud droplet riming implement in a bulk microphysics model. *J. Appl. Meteorl. Climatol.*, **47**, 694-703.

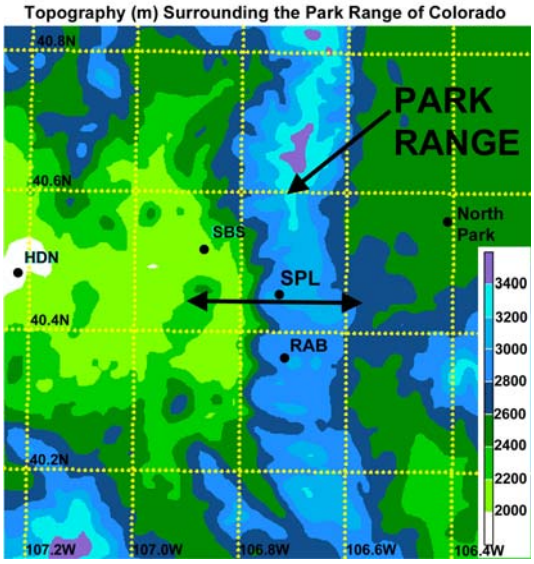

Figure 1. RAMS Grid-4 with grid spacing of 750m. Topography is overlaid (m). Locations of Hayden (HDN), Steamboat Springs (SBS), Storm Peak Lab (SPL), Rabbit Ears Pass (RAB), and North Park are labeled for reference.

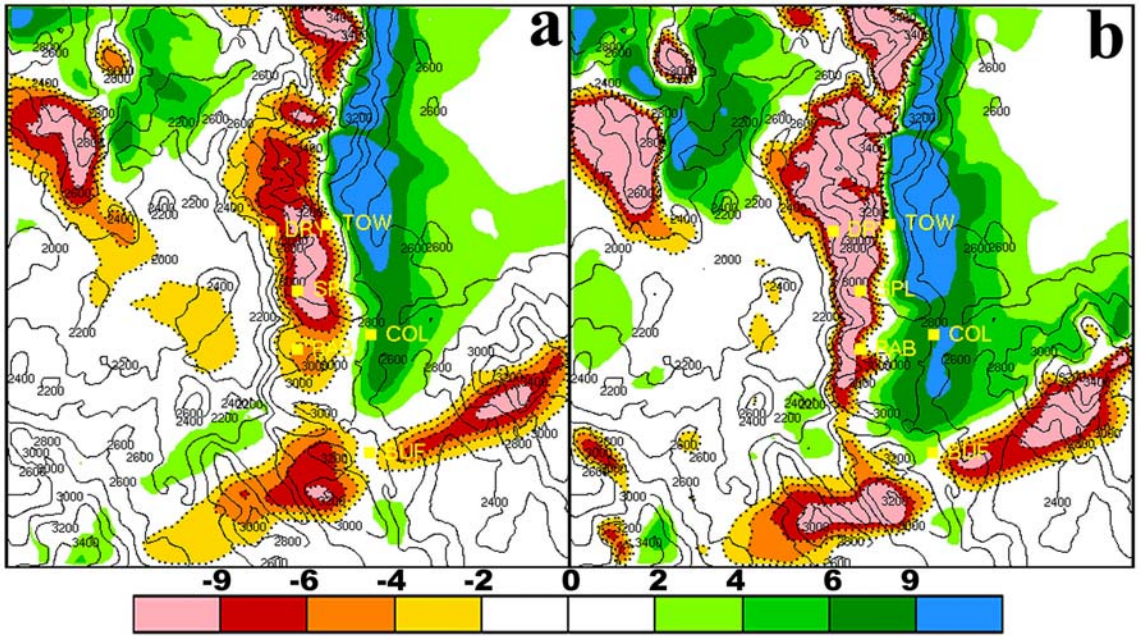

Figure 2. Accumulated SWE difference (mm) for an increase in CCN from 100 to 1900 (cm^{-3}) with GCCN held constant at: (a) 0.00001 and (b) 0.5 (cm^{-3}). Meyers IFN nucleation was used.

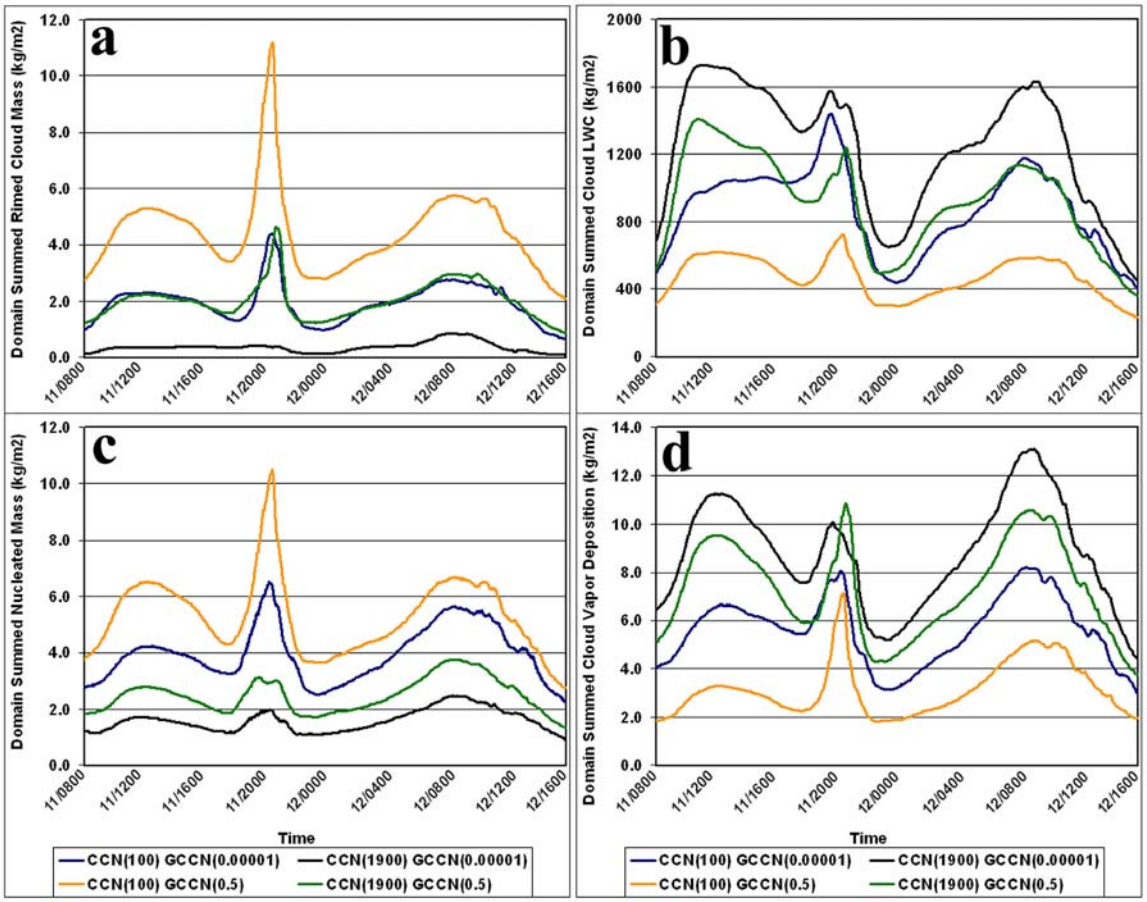

Figure 3. Time series of domain summed mass quantities of (a) rimed cloud water, (b) cloud LWC, (c) nucleated cloud water, and (d) cloud vapor deposition for varying CCN and GCCN concentration. Meyers ice nucleation was used. (Curves are identified at the bottom of the plot with the corresponding line color).

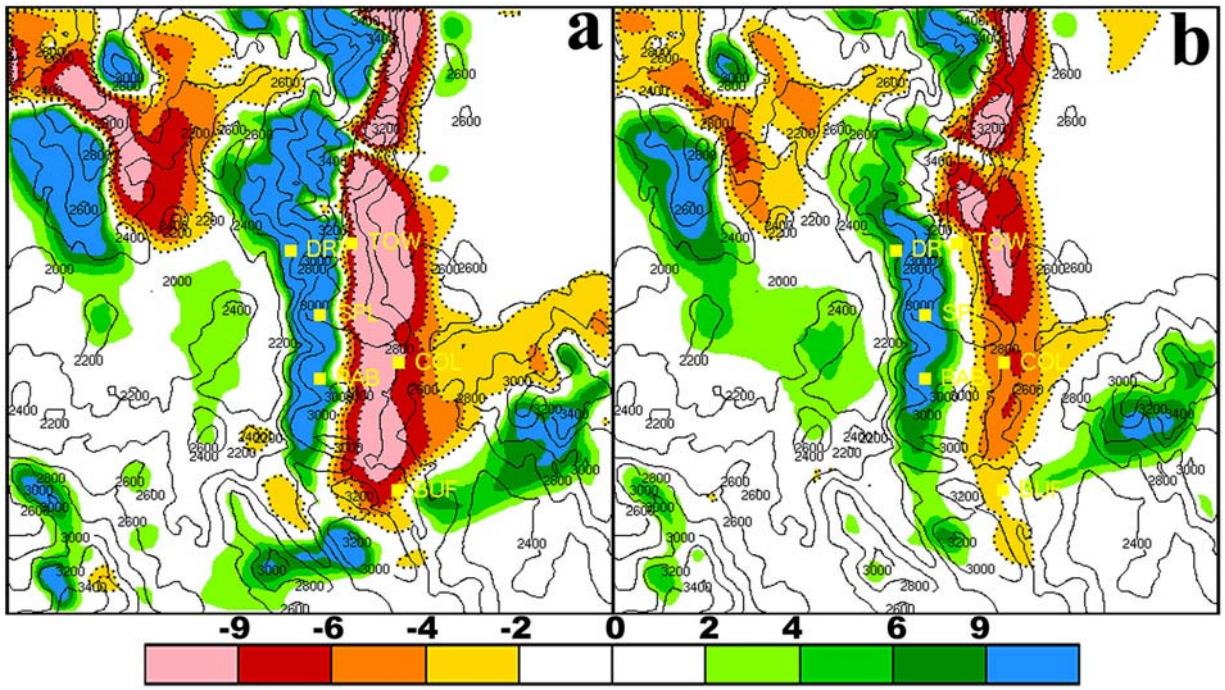

Figure 4. Accumulated SWE difference (mm) for an increase in GCCN from 0.00001 to 0.5 (cm^{-3}) with CCN held constant at: (a) 100 and (b) 1900 (cm^{-3}). Meyers IFN nucleation was used.

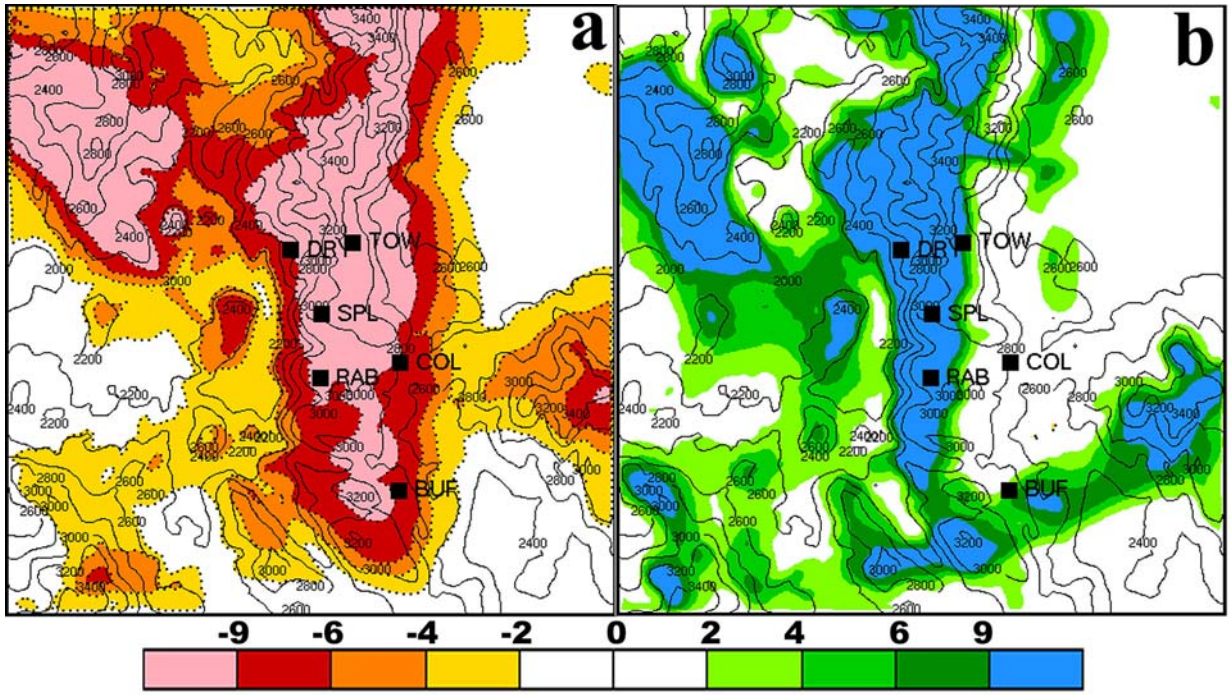

Figure 5. Accumulated difference in SWE (mm) from (a) snow + aggregates and (b) graupel for an increase in GCCN from 0.00001 to 0.5 (cm^{-3}) with CCN held constant at 100 (cm^{-3}). Meyers IFN nucleation was used.

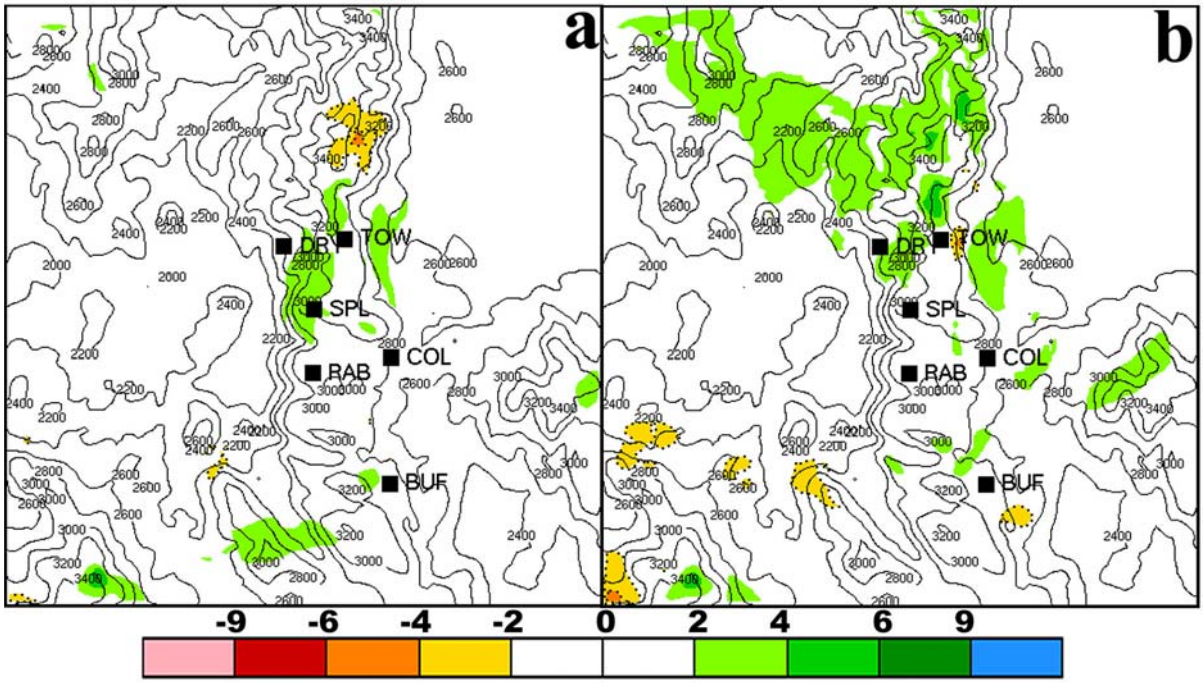

Figure 6. Accumulated SWE difference (mm) for an increase in IFN nucleation rate from the DeMott formula to the Meyers formula with GCCN held constant at 0.00001 (cm^{-3}) and CCN held constant at (a) 100 and (b) 1900 (cm^{-3}).

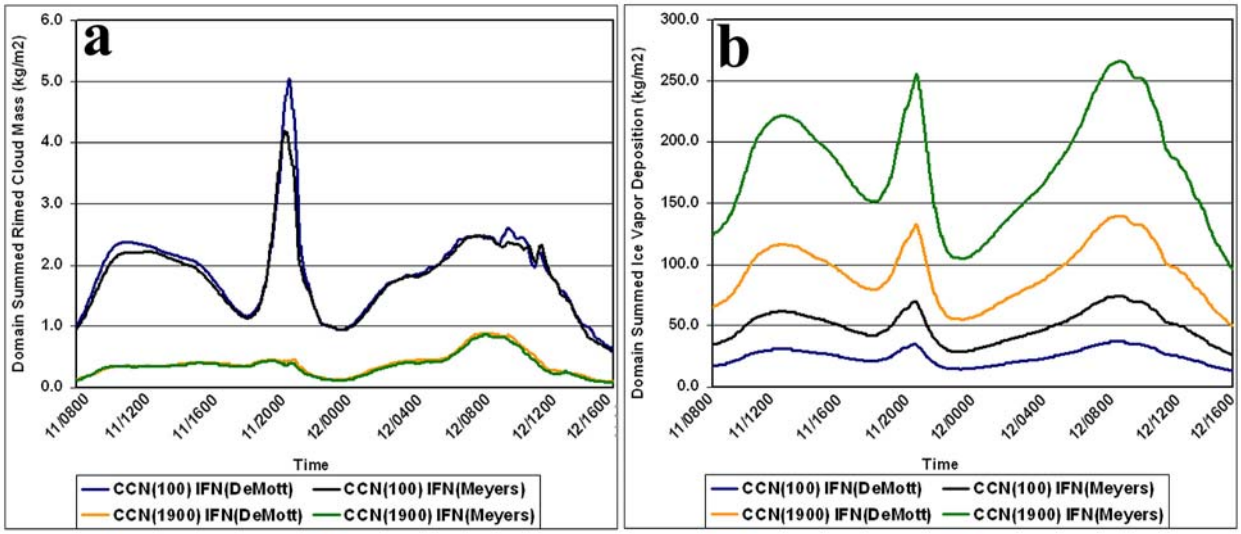

Figure 7. Time series of domain summed mass quantities of (a) rimed cloud water and (b) ice vapor deposition for varying CCN and IFN concentration. GCCN concentration is held constant at 0.0001 cm^{-3}. (Curves are identified at the bottom of the plot with the corresponding line color).